

Transport Mechanisms in Dielectric Optical Microcavities



G. Painchaud-April, J. Poirier and L. J. Dubé

Département de Physique, de Génie Physique, et d'Optique, Université Laval, Québec, Canada

Optical 2D microcavities have become a source of promising new technologies over the last decades. Applications ranging from high accuracy spectrometry to laser design will benefit from the development of such devices. The versatility of the concept resides in the ray-wave correspondence: the short wavelength limit of the system exhibits properties of well known billiard systems, which may include Hamiltonian chaos. Therefore, since the wave behaviour of an optical microcavity is influenced by the underlying phase-space structure, a study and characterization of this structure becomes important to predict where the electromagnetic energy will flow out of the cavity. Whereas the correspondence works reasonably well for regular (classically integrable) and completely chaotic systems, partially chaotic systems of mixed phase space show transport properties largely influenced by tunnelling and localization effects with the consequence that the correspondence is all but lost. We will present the results of our investigations, in the ray and wave dynamics, in order to shed some light on the collaborating influence of the different transport mechanisms.

System description

From Maxwell's equations, we get for **source-free, lossless, non-magnetic, isotropic** and **time-independent** medium of electrical permittivity $\epsilon(\mathbf{r}) = n^2(\mathbf{r})\epsilon_0$ the wave equation for the electric field $\hat{\mathbf{E}}(\mathbf{r}, t)$. Following time frequency (Fourier) expansion of $\hat{\mathbf{E}}(\mathbf{r}, t)$, we obtain a monochromatic expression of that equation. For **optically thin systems** in the z direction, the reduced wave equation is restricted to the plane $\mathbf{r} \in \mathbb{R}^2$ giving rise to 2 polarization states:

- **Transverse Magnetic (TM):** $\mathbf{E} = E_z(\mathbf{r})\hat{\mathbf{z}}$
- **Transverse Electric (TE):** $\mathbf{H} = H_z(\mathbf{r})\hat{\mathbf{z}}$

In what follows, we define $\psi \equiv E_z$ and discuss only **TM states** whose associated electric field $\psi(\mathbf{r})$ is solution of **Helmholtz equation**

$$[\nabla^2 + n^2(\mathbf{r})k^2] \psi(\mathbf{r}) = 0 \quad . \quad (1)$$

Given a domain $\Omega_c \subset \mathbb{R}^2$, the **cavity**, the boundary conditions (BCs) imposed on (1) distinguish 2 different systems:

- **Closed systems:**

Dirichlet BCs, $\psi|_{\partial\Omega_c} = 0$,

- **Open systems:**

Continuity, $\psi|_{\partial\Omega_c^+} = \psi|_{\partial\Omega_c^-}$;

Normal derivative continuity, $\partial_n\psi|_{\partial\Omega_c^+} = \partial_n\psi|_{\partial\Omega_c^-}$.

Solving Helmholtz equation in the first case results in the construction of a **discrete set** of eigenmodes $\{\psi_m\}$ existing at specific values $k = \{k_m\} \in \mathbb{R}$. In contrast, for open systems, **resonant states** appear at complex values of $k = \{k_m\} \in \mathbb{C}$. Here, we focus our attention on closed system.

Geometrical optics

In the large wavenumber limit $k \rightarrow \infty$ (**ray optics**), the dynamics of the field becomes of **hamiltonian type**. Boundary conditions are imposed to obtain (see Fig. 1)

- **Specular Reflection:** $\sin \chi_i = \sin \chi_r$
- **Refractive Transmission:** $n_{\text{in}} \sin \chi_i = n_{\text{ex}} \sin \chi_t$

Trajectories are mapped on a Poincaré section on $\partial\Omega_c$ by an impact position coordinate, arclength s (or polar angle ϕ), and momentum $p = \sin \chi_i$ (see Fig. 1). This system is formally named "**billiard**" or "**refractive (dielectric) billiard**" in the open case.

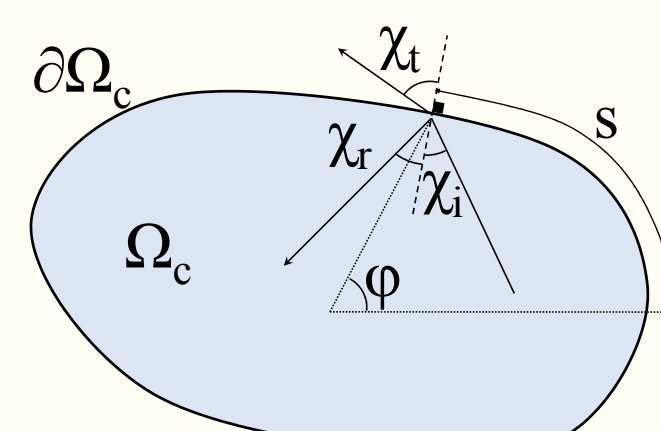


Fig. 1: Angles' definition at impact coordinate s or ϕ and incident angle χ_i .

The refraction relation defines the **total internal reflection critical angle**

$$\sin \chi_{\text{crit}} \equiv n_{\text{ex}}/n_{\text{in}} \quad . \quad (2)$$

This angle separates phase space in two distinct regions:

- **Reflective region** $|p| > \sin \chi_{\text{crit}}$: field amplitude does not suffer any loss,
- **Emission region** $|p| \leq \sin \chi_{\text{crit}}$: field gets refracted outside the cavity.

With regards to technological applications of billiard systems (e.g. lasers or sensors) one will require information about the refractive escape (emission) window. This is the reason why the **transport properties** (from the reflection to the emission region) is of central importance.

Husimi distribution

In order to establish a correspondence between the classical phase space and the modal wave solutions of Helmholtz equation (1), we need to construct a **quantum distribution function** that projects a given mode $\psi_m(\mathbf{r})|_{\partial\Omega_c}$ into phase space. Specifically, we use the **Husimi distribution function** $F^H(s, p)$ well suited for the purpose: it is positive and bounded everywhere and behaves much like a probability distribution. Adapted to the billiard system, it reads

$$F^H(s, p) \sim \left| \int_{-\infty}^{+\infty} ds' \beta^*(s - s'; p) \psi(s') \right|^2 \quad (3)$$

where

$$\beta(s; p) \sim \exp \left[-\left(\frac{s}{2\Delta s} \right)^2 \right] \exp \left(-i \frac{sp}{2\Delta s \Delta p} \right) \quad . \quad (4)$$

The Husimi distribution may be interpreted as a **gaussian smoothing** of the wave function.

Numerical results

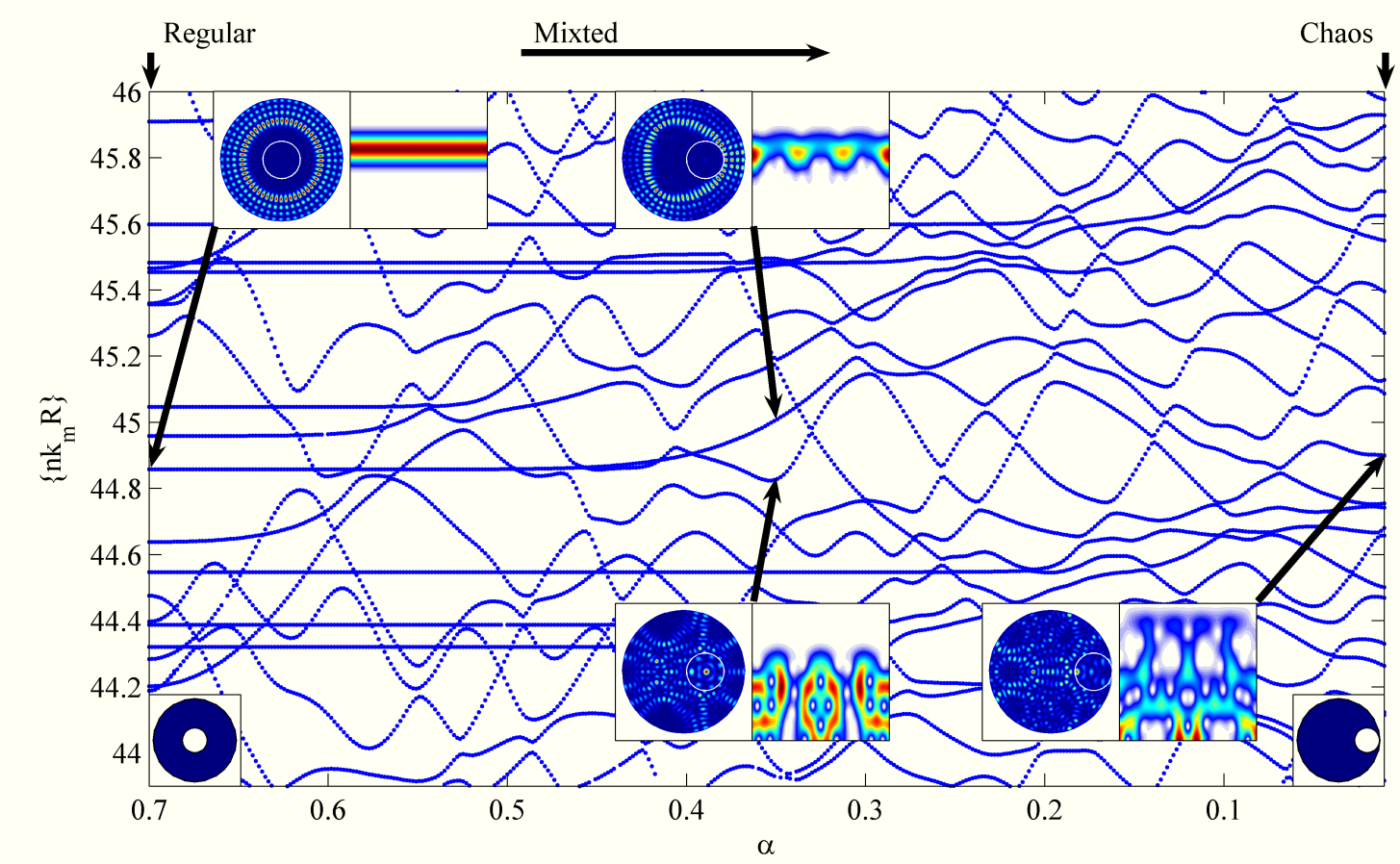


Fig. 3: Eigenvalues of equation (1) with Dirichlet BCs for annular billiard and continuous decrease of α . Typical modes and corresponding Husimi distribution for 3 different α values are shown. $n_{\text{in}} = 1.5$, $n_{\text{hole}} = 1$, $R_0 = 1$, $R_1 = 0.3$.

Parametric change leads to complex eigenvalue interactions: Fig. 3 presents many **avoided crossings** on all scales for the annular cavity (see Fig. 4).

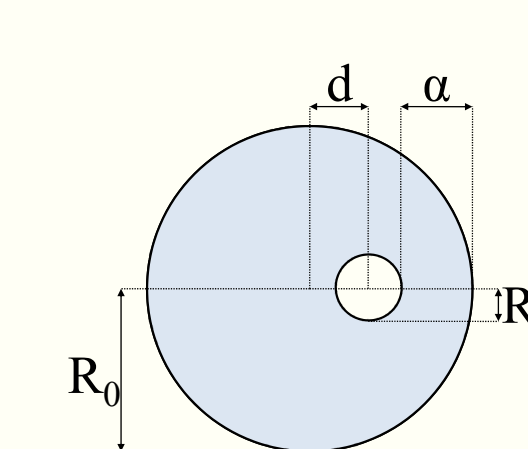


Fig. 4: Construction of annular cavity.

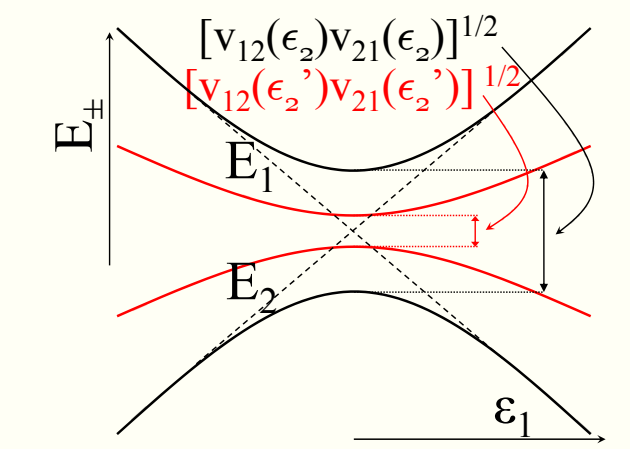


Fig. 5: Typical local behaviour between two modes in non-integrable region.

Focusing on a specific avoided crossing between two eigenvalue levels, we find typical hyperbolic curves in term of parameter ϵ_1 (Fig. 5) as

$$E_{\pm}(\epsilon_1) = \frac{E_1 + E_2}{2} \pm \sqrt{\left(\frac{E_1 - E_2}{2} \right)^2 + v_{12}v_{21}} \quad (5)$$

where locally $E_1 \propto -\epsilon_1$ and $E_2 \propto +\epsilon_1$. $E_{\pm}(\epsilon_1)$ curves are in fact eigenvalues of matrix

$$\mathbf{M} = \begin{pmatrix} E_1 & v_{12} \\ v_{21} & E_2 \end{pmatrix} \quad . \quad (6)$$

where interaction (**transport**) elements $\{v_{12}, v_{21}\}$ are related to **splitting size** between E_+ and E_- . $\{v_{12}, v_{21}\}$ may in turn depend on other parameters or interactions with **other neighboring levels** [1]. Therefore, identifying changes in separation size may be evidence of coupling (**transport**) with a third mode. This behaviour is captured in Fig. 6 where splitting size between two modes is enhanced with the proximity of a third mode.

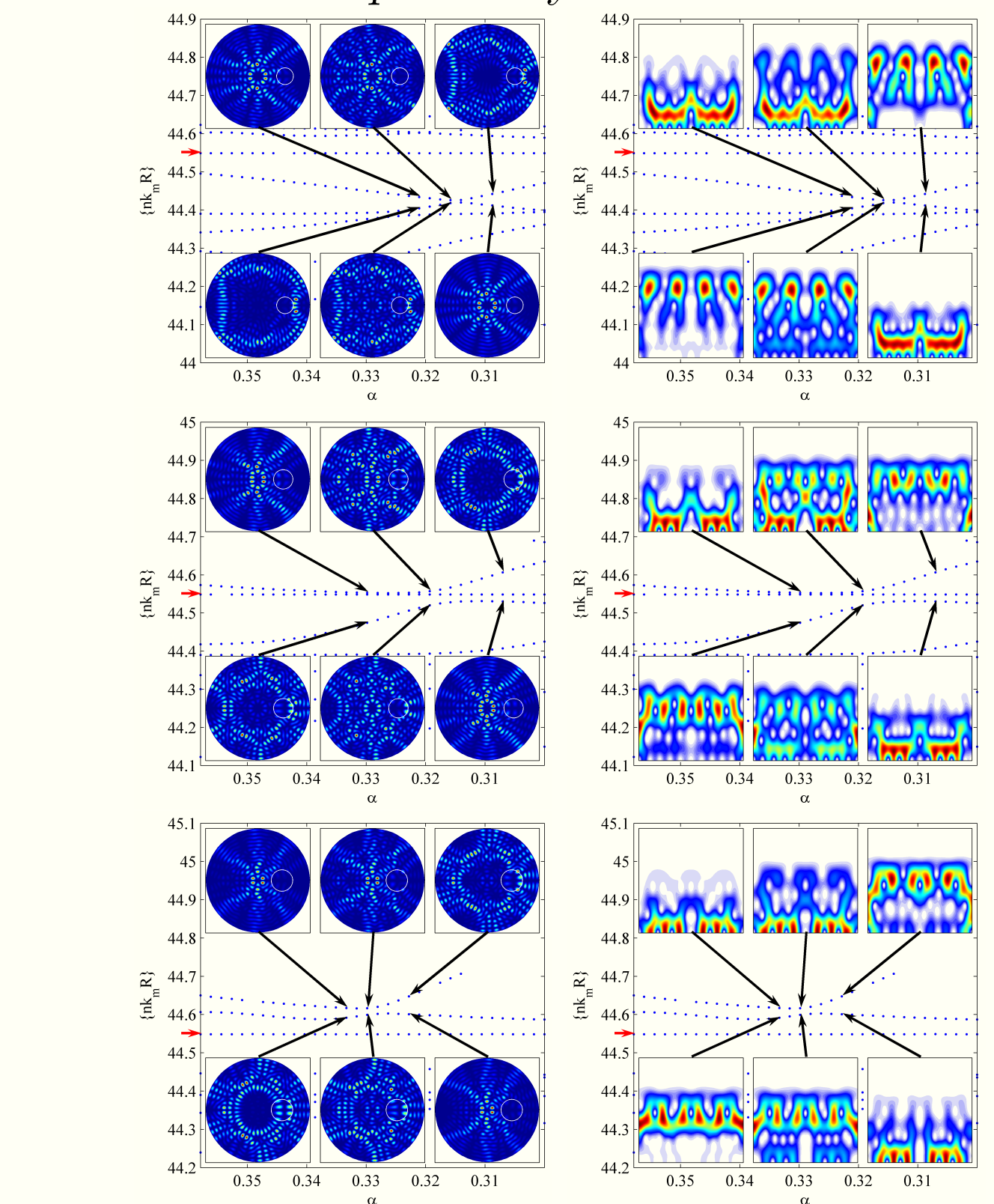


Fig. 6: Local behaviour of eigenvalues for 3 values of R_1 : Top to bottom, $R_1 = \{0.160, 0.185, 0.205\}$. Splitting size increases (more coupling) in neighborhood of a third mode (indicated by the red arrow). Left column insets present real space modes while right column insets show corresponding Husimi distributions.

[1] S. Tomsovic, J. Phys. A: Math. Gen., **31** (1998), 9469-81

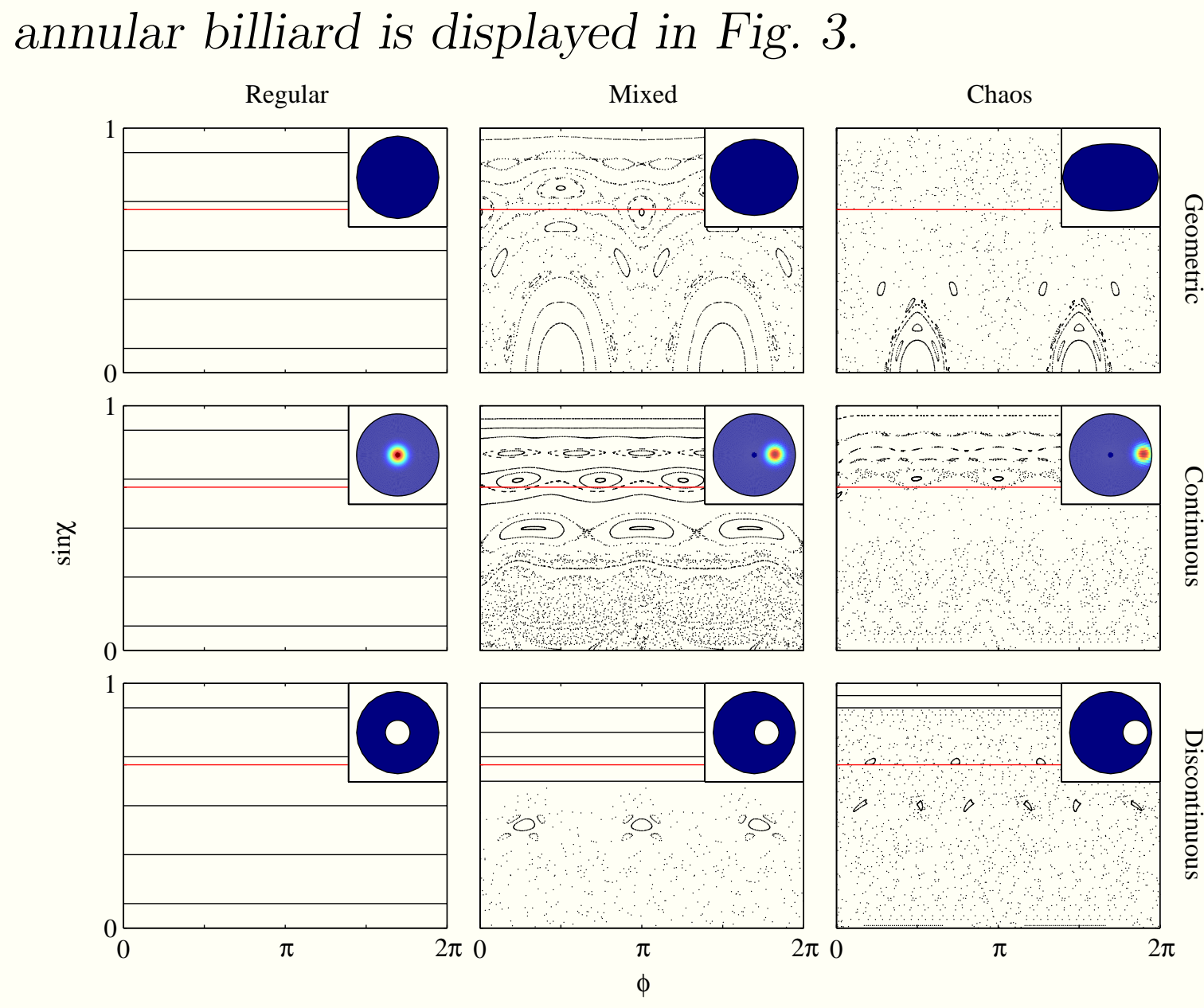


Fig. 2: Classical phase space for geometrical (quadrupolar) and inhomogeneous continuous (gaussian) and discontinuous (annular) deformations.